7-4-2001

Magnetic states of granular layered CoFe-Al_2O_3

J.B. Sousa
IFIMUP, Faculdadede Ciencias, Universidade do Porto, Rua do Campo Alegre Porto, Portugal

G.N. Kakazei
Institute of Magnetism NAS of Kiev, Ukraine

Y.G. Pogorelov
Universidade do Porto, Rua do Campo Alegre, Portugal.

J.A.M. Santos
IFIMUP, Faculdadede Ciencias, Universidade do Porto, Rua do Campo Alegre Porto, Portugal

O. Petracic
Laboratorium für Angewandte Physik, Gerhard-Mercator-Universität, Duisburg, Germany

See next page for additional authors

Magnetic States of Granular Layered CoFe–Al_2O_3 System

J. B. Sousa, G. N. Kakazei, Yu G. Pogorelov, J. A. M. Santos, O. Petracic, W. W. Kleemann, Ch. Binek, S. Cardoso, P. P. Freitas, M. M. Pereira de Azevedo, N. A. Lesnik, M. Rokhlin, and P. E. Wigen

***Abstract*—The granular layered magnetic system $Co_{80}Fe_{20}(t)/Al_2O_3$(3 nm), where the $Co_{80}Fe_{20}$ layers of nominal thickness t form separate, almost spherical magnetic granules of typical diameter 2–3 nm between the Al_2O_3 spacers, was studied. We discuss measurements of the dc and ac magnetic susceptibility χ for 1 nm $< t <$ 1.3 nm at temperatures 10 K $< T <$ 300 K and ac frequencies 0.01 Hz $< f <$ 10^3 Hz, revealing a rich variety of magnetic states, including superparamagnetic (SPM), ferromagnetic (FM)-like, and glass (G)-like. In order to describe the ac response in this disordered planar system, a generalization of the Néel–Brown approach is proposed, including random anisotropy and random molecular fields acting on the granules. The observed magnetic states are summarized in a phase diagram in the variables $t - T$, which is explained through the competition of thermal energy with two kinds of interaction between granules: usual dipolar (point-like) and FM "exchange" (due to stray dipolar fields from nonspherical granules). In particular, the coincidence of maximum low field sensitivity dMR/dH with the SPM–FM transition line on this diagram is confirmed.**

***Index Terms*—Discontinuous metal–insulator films, ferromagnetic transition, magnetic phase diagram, spin–glass transition.**

I. Introduction

DISCONTINUOUS metal–insulator multilayers (DMIM) were proposed in expectation of high sensitivity of magnetoresistance (MR) to a magnetic field H: $S = dMR/dH$, like their metal–metal predecessors [1], but much less exposed to degradation. Pioneering work on Co/SiO_2 and CoFe/HfO_2 DMIMs demonstrated their higher sensitivity compared to cermet films of the same composition and concentration [2]. Recently, we studied MR and S at room temperature (RT) as functions of nominal thickness t of ferromagnetic layer in $Co_{80}Fe_{20}(t)/Al_2O_3$(3 nm) DMIMs with $1 < t < 2.5$ nm. In particular, a sharp peak of S was observed near $t^* \approx 1.3$ nm [3]. The magnetization curves $M(H)$ for different t values displayed a crossover from SPM to FM-like behavior just above t^*, when the remanence M_r onsets in a pronounced critical way: $M_r(t) \propto (t - t^*)^{1/2}$ [4]. These anomalies in $S(t)$ and $M_r(t)$ were attributed to the so-called magnetic percolation over disconnected granules (high resolution TEM at $t \leq 1.4$ nm showed separate, nearly spherical granules with a narrow size distribution and average diameter ~3 nm).

Also, measuring MR vs T we observed the onset of hysteresis and coercivity below ~100 K in the samples with $t \leq$ 1.6 nm, increasing as temperature decreases. The increase in hysteresis is accompanied by a strong enhancement of the saturation MR value [3].

This evidence of various nontrivial magnetic states in $Co_{80}Fe_{20}(t)/Al_2O_3$(3 nm) films, important for its practical properties (like M, MR, S) motivated us to make a detailed study of the dc and ac magnetic susceptibility χ, complemented by measurements of low field MR with current-in-plane, over a wide temperature range. In parallel, theoretical models were worked out to give a consistent account of the experimental results, leading to a full phase diagram of the mentioned magnetic states, in the variables $t - T$.

II. Experimental

$[Co_{80}Fe_{20}(t)/Al_2O_3(3\text{ nm})]_{10}$ DMIMs were prepared by ion-beam deposition using methods described elsewhere [3], [4]. Susceptibility data for samples with different t were taken using a Superconducting Quantum Interference Device (SQUID) magnetometer Quantum Design MPMS-5S at temperatures $10 < T < 300$ K and ac frequencies 0.01 Hz $< f <$ 10^3 Hz at an ac amplitude $\mu_0 h = 0.4$ mT in virtually zero external field. Fig. 1 shows the data obtained for four different DMIMs at several frequencies $0.1 \leq f \leq 100$ Hz. For the $t = 1.0$ nm sample [Fig. 1(a)] $\chi'(f,T)$ and $\chi''(f,T)$ are similar to the data observed previously on frozen FeC ferrofluids [5]. A sizable dispersion in the range $40 \leq T \leq 80$ K can be associated to the onset of superspin glass (SSG) phase, while nondispersive Curie–Weiss (CW)-type decay of $\chi'(f,T)$ with an extrapolated FM Curie temperature $\Theta \approx 58$ K is encountered at $T > 80$ K [see $1/\chi'$ curves for $f = 0.1$ Hz and the best-fitted CW plot within $200 \leq T \leq 300$ K in Fig. 1(a)].

At higher nominal thickness, $t \geq 1.1$ nm, a dispersionless background appears at higher temperatures, in addition to the

Manuscript received October 13, 2000.

This work was partially supported by the program PRAXIS XXI (Portugal) through the Projects 3/3.1/MMA/1787/95, 2/2.1/FIS/302/94, P/CTM/11242/98 and the Grants BPD/3866/96 (G.N.K.) and BD/11533/97 (S.C.). This work was also supported by DFG (Graduate School "Structure and dynamics of heterogeneous systems"), DAAD (Germany) and CRUP (Portugal).

J. B. Sousa, G. N. Kakazei, and J. A. M. Santos are with IFIMUP, Faculdade de Ciencias, Universidade do Porto, Rua do Campo Alegre 687, 4169-007 Porto, Portugal. G. N. Kakazei is on leave from Institute of Magnetism NAS of Ukraine, Kiev, Ukraine (e-mail: kgleb@fc.up.pt).

Y. G. Pogorelov is with CFP and Departamento de Física, Universidade do Porto, Rua do Campo Alegre 687, 4169-007 Porto, Portugal.

O. Petracic, W. W. Kleemann, and C. Binek are with Laboratorium für Angewandte Physik, Gerhard-Mercator-Universität, 47048 Duisburg, Germany.

S. Cardoso and P. P. Freitas are with INESC, Rua Alves Redol 9-1, 1000 Lisbon, Portugal.

M. M. Pereira de Azevedo is with Departamento de Física, Universidade do Aveiro, 3810 Aveiro, Portugal.

N. A. Lesnik is with Institute of Magnetism NAS of Ukraine, 36[b] Vernadskogo blvd., 03142 Kiev, Ukraine.

M. Rokhlin and P. E. Wigen are with Department of Physics, The Ohio State University, Columbus, OH 43210 USA.

Publisher Item Identifier S 0018-9464(01)06520-7.

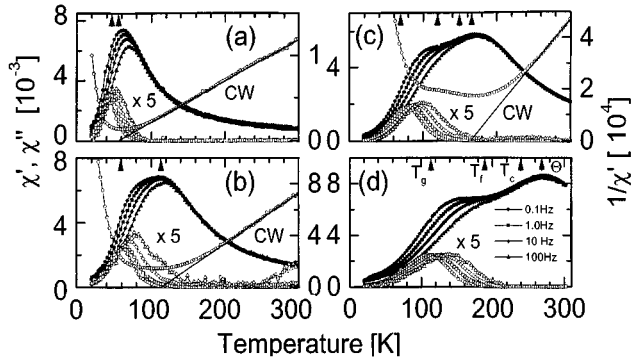

Fig. 1. $\chi'(f,T)$ and $\chi''(f,T)$ vs. T of CoFe/Al_2O_3 DMIMs with (a) t = 1.0, (b) 1.1, (c) 1.2, and (d) 1.3 nm measured at frequencies $0.1 \le f \le 100$ Hz. Note the magnification factor (5×) applicable to all χ'' data. Inverse curves $\chi'^{-1}(f = 0.1\ \text{Hz}, T)$ with best-fitted Curie–Weiss (CW) lines define the mean-field transition temperatures, Θ, as marked by arrowheads together with T_g, T_f and T_C [(c) and (d) only], so that $T_g < T_f < T_C < \Theta$.

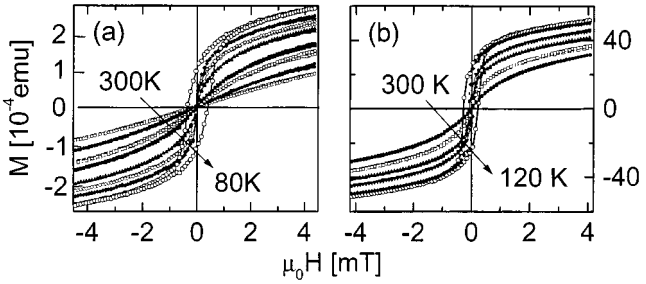

Fig. 2. Low-field magnetization curves M vs. $\mu_0 H$ obtained on the DMIM with (a) $t = 1.2$ and (b) 1.3 nm after ZFC from 300 K to (a) 300, 260, 220, 180, 140, 120, 100, and 80 K and (b) 300, 260, 220, 180, 140, and 120 K, respectively.

polydispersive response curves of the glassy subsystem at low T [Fig. 1(b)–(d)]. Its high-T tails are described by a CW law with FM mean-field Curie temperatures $\Theta(t) \approx 114$, 165 and 270 K for $t = 1.1$, 1.2 and 1.3 nm, respectively [see $1/\chi$ curves for $f = 0.1$ Hz and CW plots best-fitted above 240 K in Fig. 1(b)–(c)]. We attribute the background curves to the prevalence of FM "exchange" (due to stray dipolar fields from nonspherical granules, see below) over pure dipolar coupling [6], between "magnetically percolated" granules. Their aggregate (the infinite cluster) behaves like a FM with finite in-plane anisotropy, which causes the susceptibility to decrease upon cooling below the FM ordering temperature, $T_C < \Theta$. Notably, the dispersionless part of $\chi'(f,T)$ is not linked (through a usual scaling relation [7]) with the energy losses seen from $\chi''(f,T)$.

To clarify the nature of this FM state, which can be also called superferromagnetic (SFM) as resulting from FM ordering of SPM moments, we have measured the dc magnetization $M(H)$ in the range $-4.5 \le \mu_0 H \le 4.5$ mT. The field step was 0.1 mT for $t = 1.3$ nm and $T = 220$–260 K, but also an enhanced resolution (0.005 mT) was used at T descending from 300 K to 80 K ($t = 1.2$ nm), and to 120 K ($t = 1.3$ nm), respectively. Each of the curves (partially shown in Fig. 2) was obtained after zero-field cooling (ZFC) from 300 K. Langevin-type SPM magnetization curves are observed at high T, but upon cooling to below a certain Curie temperature T_C they develop finite jumps ΔM at $H \approx 0$. Particular T_C values were defined ≈ 150 ($t = 1.2$ nm) and 240 K ($t = 1.3$ nm). Upon further cooling $\Delta M(T)$ is growing, accordingly to the stabilization of SFM order and similarly to growing $M_r(t)$.

Obviously the SFM system behaves like a soft ferromagnet. Just below the respective T_C it is demagnetized in zero field and may be switched into its spontaneous values $\Delta M = \pm M_s$ by applying external fields in the order ± 0.1 mT. The quantity $(\Delta M/\Delta H)_{\max}$ vs T taken from the $M(H)$ curves measures SPM susceptibility at $T > T_C$. At $T < T_C$ it is proportional (within ΔH less than ± 0.1 mT) to ΔM, which is a measure of M_s.

For each t, at a certain temperature $T_f < T_C$ the $M(H)$ curve turns to be hysteretic as evidenced by finite values of M_r and coercive field H_c (Fig. 2). For instance, we defined $T_f \approx 120$ and 190 K for $t = 1.2$ and 1.3 nm, respectively. Obviously, the free energy barrier due to the weak intraplanar anisotropy is no longer overcome by thermal activation, and both M_r and H_c increase upon further cooling to below T_f. Since the T_f values roughly coincide with the onset of low-T dispersion in the ac susceptibility data [Fig. 1(c)–(d)], the observed hysteresis may be related to the metastability of the reentrant superspin glass (RSSG) phase. Indeed, there is an observable decrease of the hysteresis with waiting time t_w between the data points, e.g., in the $t = 1.3$ nm sample at $T = 150$ K H_c goes from 0.085 to 0.065 mT when t_w increases from 90 to 900 s. This suggests some link between the hysteresis and lossy dynamics of the SSG component, also seen in its frequency dispersion (Fig. 1).

Finally, under yet deeper cooling to some $T_g < T_f$ the hysteresis reaches saturation while the energy losses $\chi''(f,T)$ reach a maximum. We associate this with the SSG transition in the subsystem of magnetically nonpercolated SPM moments. Thus, the emerging SSG phase is spatially separated from the SFM phase, allowing for coexistence of the two phases in such "re-entrant" state (unlike transformation of FM into SG in usual re-entrant transitions [8]).

It is known that an independent characterization of magnetic phase states, in particular reflecting the *short-range* correlations between granule magnetic moments, can be obtained from low field MR measurements. We thus performed a detailed study of the temperature dependence $MR(T)$ at a fixed low field $\mu_0 H = 4.5$ mT [it thus scales with the field sensitivity $S(T)$] for a selected sample with $t = 1.3$ nm, the results being shown in Fig. 3. The observed maximum of $MR(T)$ near ≈ 250 K is, within experimental errors, fairly close to the above determined SPM–SFM transition temperature T_C for this sample. For comparison, the inset of Fig. 3 shows the thickness dependence $S(t)$ measured at RT, with a sharp and symmetrical peak at t^* [3]. It is clearly seen that the maximum of $MR(T)$ is much broader and has a sizable asymmetry on the two sides from T_C. The latter indicates the difference in short-range magnetic correlations for SPM and SFM states.

III. Model and Discussion

To treat the temperature dependence of ac susceptibility, we modify the known Néel–Brown approach, supposing each granule moment μ be subjected to certain random uniaxial

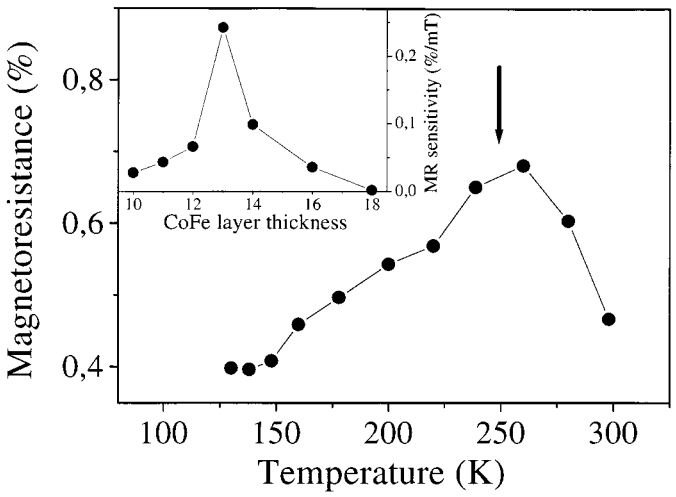

Fig. 3. Magnetoresistance of the 1.3 nm sample in a fixed applied field $\mu_0 H = 4.5$ mT as a function of temperature (the points are experimental, the line is only a guide for the eye). Estimated peak position (shown by the arrow) is about 250 K, close to the Curie temperature $T_C \approx 240$ K for this sample determined in Figs. 1 and 2.

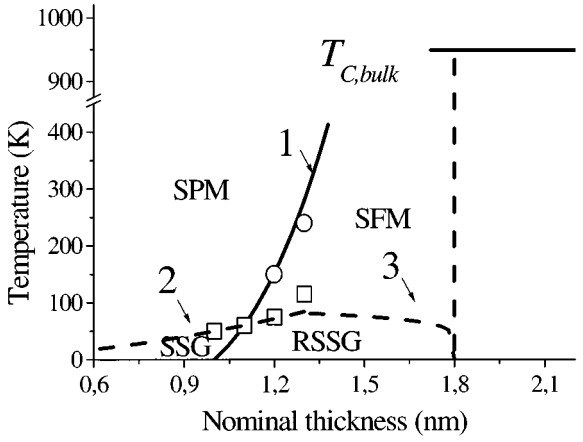

Fig. 4. Magnetic phase diagram of $Co_{80}Fe_{20}(t)/Al_2O_3$(3 nm) DMIMs in the variables t and T: (○) SPM–SFM transition by $\chi_{\rm dc}$, $\chi_{\rm ac}$ and MR data; (□) onset of SSG state, by $\chi_{\rm ac}$. Theoretical curves: (1) $T_C \propto t^2(t^2 - t_m^2)$; (2) $T_g \propto t^2$; (3) $T_g \propto (t_s - t)^{5/36}$, $T_{C,bulk} \approx 950$ K (as for bulk $Co_{80}Fe_{20}$, note the axis break).

anisotropy A and random local field $\boldsymbol{H}$, all lying in the DMIM plane, with the energy:

$$E(\theta) = A\mu^2 \sin^2\theta - \mu H \cos(\theta - \theta_H), \tag{1}$$

where θ and θ_H are respectively the angles that μ and $\boldsymbol{H}$ make with the anisotropy axis. Depending on the ratio between H and $H_A = A\mu$, the function $E(\theta)$ can have one (for $H \gg H_A$) or two (for $H \sim H_A$) minima $0 \le \theta_1 < \theta_2 \le \pi$, and in the latter case the ac field $\boldsymbol{h}_\omega(t) = \boldsymbol{h}e^{i\omega t}$, $\omega = 2\pi f$, can produce nonequilibrium occupation of the minima and give rise to energy losses. The kinetic equation for the occupation number $n_1 = 1 - n_2 \equiv n$ of the metastable minimum is:

$$\dot{n} = -(\gamma_1 + \gamma_2)\, n + \gamma_2, \tag{2}$$

where $\gamma_{1,2} = \gamma_0 \exp(-\beta h_{1,2})$, $\beta = (k_B T)^{-1}$, and the "attempt" frequency $\gamma_0 \sim 10^8$ s^{-1}. But small contributions $\sim h_\omega$ into instantaneous values of energy barriers for escape from metastable and stable minima: $h_{1,2} = h_{1,2}^{(0)} + \kappa_{1,2}\,\mathrm{Re} h_\omega$, bring some time dependence into $\gamma_{1,2}$. The general solution to (2) is:

$$n(t) = \exp\left[-\int_0^t \Gamma(t')\, dt'\right] \cdot \int_0^t \exp\left[-\int_0^{t'} \Gamma(t'')\, dt''\right] \gamma_2(t')\, dt', \tag{3}$$

with $\Gamma = \gamma_1 + \gamma_2$, and, after a waiting time $t_w \gg \Gamma^{-1}$, it attains a steady state regime $n(t) \to n_{s-s}(t)$, which is the most important in practice. It is the difference between n_{s-s} and the equilibrium value $n_0 = \{1 + \exp[\beta\Delta]\}^{-1}$ (where $\Delta = h_2^{(0)} - h_1^{(0)}$) that defines a contribution to complex ac susceptibility $\chi_{\rm ac}$:

$$\chi_{\rm ac} = \overline{h_\omega * (\kappa_1 - \kappa_2)(n_{s-s} - n_0)}/h^2, \tag{4}$$

with the average over time and orientations of random fields and anisotropies. At high enough T, such that $\gamma \gg \omega$, the steady state is simply $n_{s-s}(t) \approx \{1 + \exp[\beta\Delta(t)]\}^{-1}$ where $\Delta(t) = h_2(t) - h_1(t)$ adiabatically follows the variation of the energy levels. Then we obtain:

$$\chi_{\rm ac} = \beta\overline{(\kappa_1 - \kappa_2)^2 n_0 (1 - n_0)}, \tag{5}$$

and the self-consistency relation $\overline{H} = J\chi h_\omega$, with the above used FM "exchange" J leads to CW law with $\Theta \sim J/k_B \sim T_C$.

Equations (3) and (4) still apply for a more complicate nonadiabatic case ($\Gamma \sim \omega$) taking place at $T \sim T_g$. Here we only note that the estimate for energy barriers $\sim k_B T_g \ln(\gamma_0/\omega)$ gives $\sim k_B 10^3$ K for our system. This is too high to be accounted for by the typical interaction energy of two granules $\mu^2/a^3 \sim k_B 10^2$ K, and gives a hint that effective SPM moments (superspins) should involve up to ~10 granules.

Finally, the phase diagram of magnetic states in variables $t - T$ (Fig. 4) can be summarized as follows. The SPM–SFM transition (line 1 in Fig. 4) occurs when the dipolar interaction energy, which is continuously frustrated for point dipoles [6] or spherical granules, obtains a growing contribution from stray fields produced by nonspherical particles. The latter appear due to coalescence at growing size $d = (6ta^2/\pi)^{1/3}$ of spherical granules, nucleated at random centers with mean distance a. The relative number of coalesced granules rapidly increases with nominal thickness t as $P(t) = 1 - \exp[-(t/a)^{1/3}]$, hence their structural percolation occurs at $P(t_s) \approx 0.5$ and $t_s \approx a/3$, while the magnetic percolation begins at only slightly lower $P(t_m) \approx 0.45$ but at notably thinner $t_m \approx a/5$. The effective Curie temperature rapidly grows as $T_C(t) \propto t^2(t^2 - t_m^2)$, eventually reaching $T_C(t_s) \sim T_{C,bulk} \sim 10^3$ K when the infinite SFM cluster turns into usual FM.

A rough estimate of temperature $T_g(t)$ at $t < t_m$ is given by the mean fluctuation of dipolar field $\sim \mu^2/a^3$, resulting in its t-dependence $T_g(t) \sim (6M/\pi)^2 a t^2$ (SPM–SSG, line 2). This increase of $T_g(t)$ is limited at $t > t_m$ and drops to zero $\propto (t_s - t)^\nu$ at $t \to t_s$ (SFM–RSSG, line 3), due to vanishing

probability to find SPM clusters in almost FM medium, and this can be described, e.g., by the percolation index $\nu = 5/36$ [9].

REFERENCES

[1] B. Dieny, S. Sankar, M. R. McCartney, D. J. Smith, P. Bayle-Guillemaud, and A. E. Berkowitz, "Spin-dependent tunneling in discontinuous metal/insulator multilayers," *J. Magn. Magn. Mater.*, vol. 185, pp. 283–292, June 1998.

[2] S. Sankar, B. Dieny, and A. E. Berkowitz, "Spin-polarized tunneling in discontinuous CoFe/HfO_2 multilayers," *J. Appl. Phys.*, vol. 81, pp. 5512–5514, Apr. 1997.

[3] G. N. Kakazei, P. P. Freitas, S. Cardoso, A. M. L. Lopes, M. M. Pereira de Azevedo, Y. G. Pogorelov, and J. B. Sousa, "Transport properties of discontinuous $Co_{80}Fe_{20}/Al_2O_3$ multilayers," *IEEE Trans. Magn.*, vol. 35, pp. 2895–2897, Sept. 1999.

[4] G. N. Kakazei, Y. G. Pogorelov, A. M. L. Lopes, J. B. Sousa, S. Cardoso, P. P. Freitas, M. M. Pereira de Azevedo, and E. Snoeck, "Tunnel magnetoresistence and magnetic ordering in ion-beam sputtered $Co_{80}Fe_{20}/Al_2O_3$ discontinuous multilayers,". unpublished.

[5] T. Jonsson, P. Svedlindh, and M. F. Hansen, "Static scaling on an interacting magnetic nanoparticle system," *Phys. Rev. Lett.*, vol. 81, pp. 3976–3979, Nov. 1998.

[6] J. M. Luttinger and L. Tisza, "Theory of dipole interaction in crystals," *Phys. Rev.*, vol. 70, pp. 954–964, Dec. 1946.

[7] A. T. Ogielski, "Dynamics of three-dimensional Ising spin glasses in thermal equilibrium," *Phys. Rev. B*, vol. 32, pp. 7384–7398, Dec. 1985.

[8] B. K. Srivastava, A. Krishnamurthy, V. Ghose, J. Mattson, and P. Nordblad, "Re-entrant spin glass like behavior of $(Fe_{0.90}Cr_{0.05}Ni_{0.05})_2P$," *J. Magn. Magn. Mater.*, vol. 132, pp. 124–130, Apr. 1994.

[9] D. Stauffer, "Scaling theory of percolation clusters," *Phys. Reports*, vol. 54, pp. 1–74, 1979.